Reprinted from

JAPANESE JOURNAL OF
APPLIED
PHYSICS

REGULAR PAPER

Production of Local Acoustic Radiation Force to Constrain Direction of Microcapsules in Flow

Kohji Masuda, Nobuyuki Watarai, Ryusuke Nakamoto, and Yusuke Muramatsu

Jpn. J. Appl. Phys. **49** (2010) 07HF11

Japanese Journal of Applied Physics 49 (2010) 07HF11 **REGULAR PAPER**

Production of Local Acoustic Radiation Force to Constrain Direction of Microcapsules in Flow

Kohji Masuda*, Nobuyuki Watarai, Ryusuke Nakamoto, and Yusuke Muramatsu

Graduate School of Bio-Applications and Systems Engineering, Tokyo University of Agriculture and Technology, 2-24 Nakacho, Koganei, Tokyo 184-8588, Japan

Received November 25, 2009; revised March 31, 2010; accepted April 8, 2010; published online July 20, 2010

We have ever reported our attempt to control the direction of microcapsules in flow by acoustic radiation force. However, the diameter of capsules was too large to be applied *in vivo*. Furthermore, the acoustic radiation force affected only the focal area because focused ultrasound was used. Thus, we have improved our experiment by using microcapsules as small as blood cells and introducing a plane wave of ultrasound. We prepared an artificial blood vessel including a Y-form bifurcation established in two observation areas. Then, we newly defined the induction index to evaluate the difference in capsule density in two downstream paths. As a result, the optimum angle of ultrasound emission to induct to the desired path was derived. The induction index increased in proportion to the central frequency of ultrasound, which is affected by the aggregation of capsules to receive more acoustic radiation force. © 2010 The Japan Society of Applied Physics

DOI: 10.1143/JJAP.49.07HF11

1. Introduction

Many researches of drug delivery system have been proposed by applying microcapsules or microbubbles as a drug carrier in the human body.[1–4] The existence of capsules (or bubbles) improves the introduction efficiency to the target area by making use of sonoporation.[5] While the lifetime of the microbubbles is several minutes, we consider that the microcapsules are more suitable for use with various types of delivery. However, because of the diffusion of capsules after injection, it is difficult to deliver capsules from the point of injection to desired target area through bifurcations of blood vessel. If the behavior of capsules could be controlled and constrained in terms of direction, the introduction efficiency would be enhanced. Owing to acoustic radiation force,[6–9] which is a physical phenomenon where an acoustic wave pushes an obstacle along its direction of propagation, we have previously reported our attempt to propel microcapsules in water.[10] We have elucidated the conditions of sound pressure, flow velocity, and diameter of capsules for the active path selection of capsules in an artificial blood vessel. However, because we used capsules with diameters of more than 60 μm, they were too large to be applied *in vivo*. Furthermore, we also used focused ultrasound to concentrate the acoustic radiation force, which affected only the focal area. Because the acoustic radiation force is proportional to the square of the size of a capsule, a larger acoustic field can produce more radiation force to propel a capsule in flow. Thus, we have improved our experiment to adopt capsules as small as blood cells with a plane wave of ultrasound.

Considering micrometer-sized microcapsules, upon ultrasound exposure, they are oscillated to produce Bjerknes force and aggregate with each other[11,12] if the frequency of ultrasound is near their resonance frequency. We already confirmed the aggregation of capsules in a straight flow when acoustic radiation force was produced in the oncoming direction with MHz-order frequencies.[13] However, frequency dependence was not elucidated when capsules were propelled in flow by the radiation force.[14,15] In this study, we investigated the optimal conditions to propel microcapsules in flow using a plane wave of ultrasound with various frequencies.

*E-mail address: masuda_k@cc.tuat.ac.jp

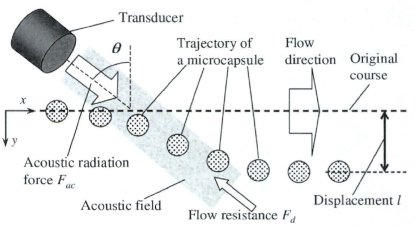

Fig. 1. Trajectory of microcapsule in flow under ultrasound emission.

2. Principle

Assuming that the shape of capsules is spherical and they are located in a uniform acoustic field, an acoustic radiation force acts to propel a capsule in the direction of acoustic propagation as per the following equation:[15,16]

$$F_{ac} = \pi r^2 Y_p P, \tag{1}$$

where P is the mean energy density of the incident wave, Y_p is a dimensionless factor called the radiation force function that depends on the scattering and absorption properties of the capsule, and r is the radius of the capsule. Here, the effect of ultrasound frequency in F_{ac} is not clear because Y_p does not include an item of frequency.[17]

When the microcapsules are placed in flow, a capsule should receive flow resistance. If the acoustic radiation force is greater than the flow resistance, the trajectory of the capsule is curved, as shown in Fig. 1. At a positive value of angle θ in Fig. 1, a capsule is propelled in the y-direction with lower flow resistance than at a negative value of angle θ. At a larger value of angle θ, although a capsule passes through the acoustic field for a longer period, the radiation force propels the capsule in the x-direction more than in the y-direction. In Fig. 1, although the shape of the acoustic field is expressed as a square, it is measured before the experiment.

3. Experimental Methods

3.1 Diameter distribution of microcapsules

We used F-04E microcapsules (Matsumoto Oil), which have

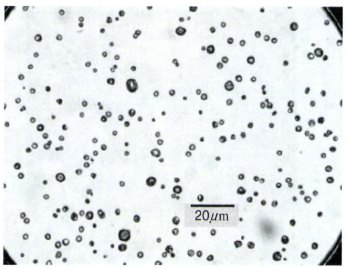

Fig. 2. Microscope image of selected F-04E microcapsules with a diameter of less than 5 μm.

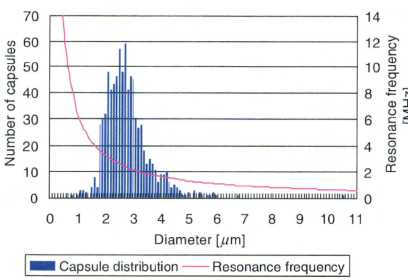

Fig. 3. (Color online) Diameter distribution of F-04E microcapsules plotted with the resonance frequency of eq. (2) according to the diameter.

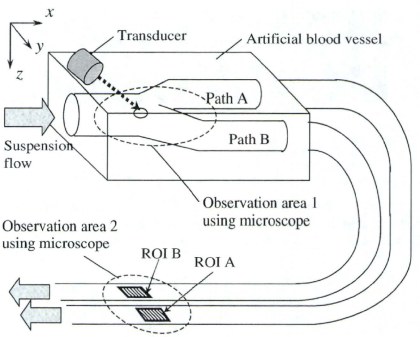

Fig. 4. Schematic view of artificial blood vessel with the locations of the two observation areas.

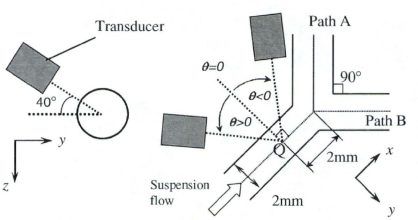

Fig. 5. Position configuration between a transducer and the artificial blood vessel near the bifurcation.

a shell made of poly(vinyl chloride) (PVC), a specific gravity of 0.0225, and an average diameter of 4 μm. They contain isobutene inside and are stable at room temperature. We selected only those microcapsules with a diameter of less than 5 μm by using microsieves. Figure 2 shows a microscope image of the selected microcapsules. We measured the diameter of more than 800 capsules through five microscope images to elucidate the diameter distribution of the capsules. Figure 3 shows the diameter distribution of the capsules as bars, where most of the diameters of capsules are between 2 and 3.5 μm. Since the solid line in Fig. 3 indicates the resonance frequency f of the microbubble, which is calculated as per eq. (2),[7,18] the resonance frequency ranges between 2 and 4 MHz according to the diameter.

$$f = \frac{1}{2\pi r}\sqrt{\frac{3kP}{\rho}}, \tag{2}$$

where k is the ratio of specific heats. However, because of the shell, the resonance frequency of microcapsules should be higher than that of microbubbles. According to a mathematical simulation,[19] the theoretical resonance frequency of microcapsules is estimated to be between 5 and 7 MHz with a diameter of 4 μm. Thus, the behavior of capsules is considered to be mostly affected by MHz-order frequencies.

3.2 Observation of capsule behavior

We have also prepared an artificial blood vessel made of poly(ethylene glycol) (PEG), including a Y-form bifurcation, as shown in the schematic view of Fig. 4. The external size was $85 \times 55 \times 10\,\mathrm{mm}^3$ and the inner diameter of the paths was 2 mm. The blood vessel was placed in the bottom of a water tank, which was filled with water. Because the acoustic impedance of PEG (sound velocity: 1540–1560 m/s, density: 1.27 g/mL) is similar to that of water, the energy of ultrasound in water reaches the path with high efficiency. As shown in Fig. 4, optical images of observation areas 1 and 2 were recorded independently using a microscope (Omron KH-7700) and an inverted microscope (Leica DMRIB), respectively.

Figure 5 shows the position configuration between a transducer and the artificial blood vessel near the bifurcation in observation area 1. The axis of the transducer was set at 40° from the $-y$ direction around the x-axis to prevent physical interference between the transducer and the edge of the water tank. The transducer included a flat ceramic disc with a diameter of 20 mm to emit a plane wave of ultrasound. We have prepared five transducers, which have their central frequencies at 0.5, 1, 2, 3, and 5 MHz, to compare the effect of resonance frequency. Figure 6 shows the two-dimensional distribution of sound pressure of the 3 MHz transducer, where the x-axis indicates the direction of

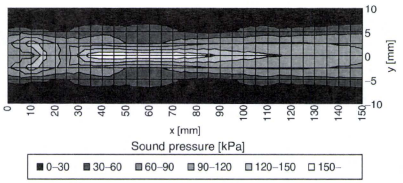

Fig. 6. Two-dimensional distribution of sound pressure of the 3 MHz transducer. (x-axis indicates the direction of ultrasound propagation, and the line of $x = 0$ corresponds to surface of the transducer).

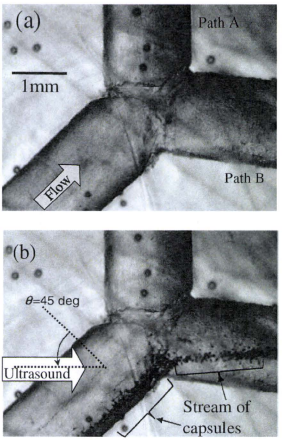

Fig. 7. Comparison of microscope images of observation area 1 (a) before and (b) after injection of capsule suspension (flow velocity: 20 mm/s, central frequency of ultrasound: 2 MHz, and maximum sound pressure: 400 kPa).

ultrasound propagation, and the line of $x = 0$ corresponds to the surface of the transducer. The shape of the highest sound pressure is wider than that of focused ultrasound.[10] Because the half width of the ultrasound beam ranges between 4 and 5 mm in above five transducers, the axis of the transducer was directed to point Q, as shown in Fig. 5, which was set to be 2 mm from the bifurcation point to the upstream course. The distance from the surface of a transducer to point Q was set to between 50 and 60 mm, so that point Q is included in the area of the highest sound pressure.

3.3 Evaluation of induction of capsules to the desired path

As shown in Fig. 7, when ultrasound was emitted, aggregations of capsules were clearly observed to enter path B rather than path A in observation area 1, whereas neither aggregations of capsules nor a significant difference between paths were observed without ultrasound. To evaluate the number of capsules that passed through each path, we extended the two paths using semitransparent tubes and

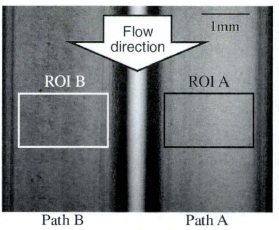

Fig. 8. Microscope images of observation area 2, which were taken at 300 fps after the injection of the capsule suspension in a flow velocity of 5 mm/s with an ultrasound emission of 2 MHz and a maximum sound pressure of 500 kPa.

established observation area 2, where both paths were observable in a single view. Figure 8 shows microscope images of observation area 2, which were captured using a high-speed camera (Casio EX-F1) attached to the microscope with an interval time of 3.3 ms (300 fps), when the capsule suspension was injected with a flow velocity of 5 mm/s with ultrasound emission of 2 MHz, and a maximum sound pressure of 500 kPa. Because of the limitation of optical magnification, although individual microcapsules cannot be distinguished, thicker suspension in path B was confirmed.

To measure the amount of microcapsules, we established two square regions of interest (ROI), the size of which is $1.8 \times 1.2\,\mathrm{mm}^2$, in each path (ROIs A and B) and calculated the average brightness. In our previous paper[10] we evaluated the amount of capsules by defining the shadow index, which reflects the brightness change according to the existence of capsules in a ROI. However, the value of the shadow index cannot be compared between ROIs if there is an initial brightness difference between them. Thus, we newly defined the induction index by comparing two ROIs as follows.

Figure 9 shows the variations in brightness average in both ROIs upon injection of a capsule suspension with a flow velocity of 20 mm/s. Before the injection, the brightness was constant but there was a difference between the two ROIs. According to the appearance of capsules, after 7 s, the brightness of both ROIs decreased simultaneously. A significant different variation was confirmed upon ultrasound emission of 2 MHz and 500 kPa, which indicates that more capsules were inducted to ROI B after 28 s. According to disappearance of capsules, after 48 s, they returned to their initial brightness. Thus, calculating the subtraction of brightness with capsules from the initial brightness in each ROI, and comparing ROIs, we have defined the induction index ξ_B (%) of capsules to be inducted to path B rather than path A using the following equation:

$$\xi_B = \frac{(I_B - I_{B0}) - (I_A - I_{A0})}{(I_B - I_{B0}) + (I_A - I_{A0})} \times 100, \tag{3}$$

where I_{A0} and I_{B0} indicate the initial brightness average without capsules, and I_A and I_B indicate the brightness average with capsules, in ROI A and B, respectively. We confirmed that the induction index ξ_B reflects the relative ratio of capsules to pass through ROI B versus the total

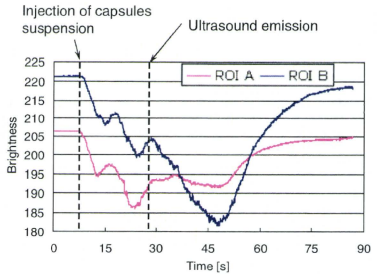

Fig. 9. (Color online) Variations in brightness average in ROIs A and B upon injection of a capsule suspension with a flow velocity of 20 mm/s, before and after ultrasound emission of a maximum sound pressure of 500 kPa and central frequency of 2 MHz.

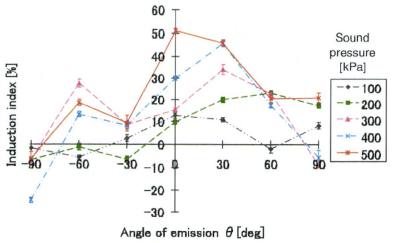

Fig. 10. (Color online) Induction index versus angle of emission with plane ultrasound of 3 MHz and flow velocity of 20 mm/s.

amount of capsules through our previous recordings movies,[10,13] in which we calculated the shadow index versus capsules density.

4. Results and Discussion

Figure 10 shows the induction index ξ_B versus the angle of ultrasound emission θ for five types of maximum sound pressure, a flow velocity of 20 mm/s, and a central frequency of 3 MHz. Here, the value of induction index was calculated from the sampled frames recorded with a high frame of 300 fps, while capsules appeared in the frame under ultrasound emission. The number of sampled frames was set to 300 frames, which depends on the duration of capsule appearance. When the sound pressure is less than 200 kPa, dominant induction to path B was observed in the positive angle of emission. When the sound pressure is more than 300 kPa, although capsule induction to path B was confirmed at an angle of emission of $-60°$, significant induction to path B was confirmed at an angle of emission of 30°. The optimum angle of ultrasound emission for induction to path B in the experiment was at an angle of 30°, which was used in the following experiment.

We measured the induction index upon emission of sinusoidal ultrasound with frequencies of 0.5, 1, 2, 3, and 5 MHz. Figures 11(a)–11(c) show the values of the induction

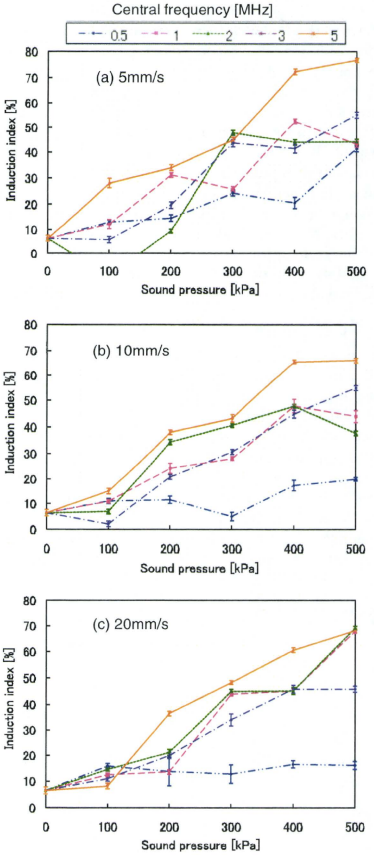

Fig. 11. (Color online) Induction index versus maximum sound pressure of plane ultrasound by the angle of emission of 30° in flow velocities of (a) 5, (b) 10, and (c) 20 mm/s, respectively.

index versus the maximum sound pressure, when the flow velocity was 5, 10, and 20 mm/s, respectively, where θ was fixed at 30°. Under every condition of flow velocity, the induction index increased in proportion not only to the sound pressure but also to the central frequency of the ultrasound. Regarding the central frequency, more capsules were inducted to the desired path when it was close to the resonance frequency, which is considered to be more than 5 MHz. We have considered that the result reflects the effect of aggregation of capsules.

Because capsules form aggregations under ultrasound emission, they should be equivalent to a larger volume than isolated capsules. When the frequency is near the resonance frequency, the capsules would be greatly oscillated to form

larger aggregations and to receive more acoustic radiation force in the direction of propagation. We have to investigate the behavior of capsules more precisely under various conditions of ultrasound.

From these results, using the higher pressure, higher frequency, and plane ultrasound, more capsules could be inducted to the desired path at the bifurcation of a blood vessel. In the next step, we are going to elucidate the behavior of capsules in flow theoretically before applying it to an *in vivo* experiment. The effect of acoustic streaming should be considered by using a higher frequency than 5 MHz. Meanwhile, we are going to develop a method to identify the precise location of bifurcations *in vivo* by detecting and constructing the three-dimensional shape of the blood vessel.

5. Conclusions

In this study, we realized active control of microcapsules with a diameter of less than 5 μm to constrain the direction in an artificial blood vessel. In a simple bifurcation, significant induction was confirmed when the angle of ultrasound emission was 30° from the rectangular of the flow to upstream. We confirmed that capsules were inducted into the desired path using the higher pressure, higher frequency, and plane ultrasound. For further analysis, the precise conditions necessary to realize active control of capsules in a complicated shape of blood vessel should be elucidated. Also, we are going to consider applications for future *in vivo* experiments.

Acknowledgment

This work was supported by Research and Development Committee Program of the Japan Society of Ultrasound in Medicine.

1) M. Watanabe, K. Chihara, K. Shirae, K. Ishihara, and A. Kitabatake: *Proc. 11th Symp. Ultrasonic Electronics, Kyoto, 1990*, Jpn. J. Appl. Phys. **30** (1991) Suppl. 30-1, p. 241.
2) N. de Jong, R. Cornet, and C. T. Lancée: Ultrasonics **32** (1994) 447.
3) K. Okada, N. Kudo, K. Niwa, and K. Yamamoto: J. Med. Ultrason. **32** (2005) 3.
4) H. Zheng, P. Dayton, C. Caskey, S. Zhao, S. Qin, and K. Ferrara: Ultrasound Med. Biol. **33** (2007) 1978.
5) Y. Yamakoshi, Y. Koitabashi, N. Nakajima, and T. Miwa: Jpn. J. Appl. Phys. **45** (2006) 4712.
6) Y. Yamakoshi: Jpn. J. Appl. Phys. **40** (2001) 1526.
7) H. Mitome: Jpn. J. Appl. Phys. **40** (2001) 3484.
8) T. Kozuka, K. Yasui, T. Tuziuti, A. Towata, and Y. Iida: Jpn. J. Appl. Phys. **47** (2008) 4336.
9) T. Kozuka, K. Yasui, T. Tuziuti, A. Towata, J. Lee, and Y. Iida: Jpn. J. Appl. Phys. **48** (2009) 07GM09.
10) K. Masuda, Y. Muramatsu, S. Ueda, R. Nakamoto, Y. Nakayashiki, and K. Ishihara: Jpn. J. Appl. Phys. **48** (2009) 07GK03.
11) Y. Yamakoshi and T. Miwa: Jpn. J. Appl. Phys. **47** (2008) 4127.
12) Y. Yamakoshi and T. Miwa: Jpn. J. Appl. Phys. **48** (2009) 07GK02.
13) K. Masuda, R. Nakamoto, Y. Muramatsu, Y. Miyamoto, K. Kim, and T. Chiba: Proc. 31st Annu. Int. Conf. IEEE Engineering in Medical and Biology Society, 2009, p. 295.
14) T. Lilliehorn, U. Simu, M. Nilsson, M. Almqvist, T. Stepinski, T. Laurell, J. Nilsson, and S. Johansson: Ultrasonics **43** (2005) 293.
15) T. Hasegawa, Y. Hino, A. Annou, H. Noda, and M. Kato: J. Acoust. Soc. Am. **93** (1993) 154.
16) F. G. Mitri: Wave Motion **43** (2005) 12.
17) T. Hasegawa, T. Kido, C. W. Min, T. Iizuka, and C. Matsuoka: Acoust. Sci. Technol. **22** (2001) 273.
18) M. Minnaert: Philos. Mag., Ser. 7 **16** (1933) 235.
19) K. Yasui, J. Lee, T. Tuziuti, A. Towata, T. Kozuka, and Y. Iida: J. Acoust. Soc. Am. **126** (2009) 973.

0916-2410/10/¥500/論文/JCLS
U0908-07

解　説　　医用超音波

模擬血管中を流れるマイクロカプセルに対する音響放射力とその影響

＝超音波による薬物伝送システム（DDS）のための基礎検討＝

東京農工大学　村松 悠佑・桝田 晃司

1. はじめに

現代の医療にとって投薬治療は必要不可欠な方法として用いられている反面、投薬効率や副作用など解決すべき問題も存在する。そのため、患部にのみ必要量の薬物を送る選択的薬物伝送システム（Drug Delivery System, DDS）の研究が注目されている。現在の主流は修飾基等による化学的DDSであるが、開発にかかる時間とコストが膨大で、しかも汎用性に乏しいという欠点がある[1]。それに対して中空マイクロカプセル中に薬物を含ませ、患部に届ける物理的DDSの研究も進められている[2]~[4]。

この方法は、薬物を含むマイクロカプセルを患部に届け、体外からの超音波照射によってカプセルを破壊することで目的部にのみに投薬を行う。カプセルに含まれる気体は血液中では優れた超音波感受性を持つため、体外からのモニタリングが容易であり、カプセルの検出と破壊を超音波のみによって行うことが出来る。またこの手法を化学的DDSと組み合わせることにより、カプセルに含ませる薬物を替えるだけで様々な投薬治療を低コストで行うことが出来るだけでなく、将来的には遺伝子導入[5]も可能になると考えられる。最近では、抹消血管さえも通過することが出来るマイクロカプセルが開発されている[6]ため、実現性は高いと考えられる。超音波とマイクロカプセルを用いたDDS実現のためには大きく分けて以下の４つの技術が必要になる。

① 多くのカプセルを目的部に誘導する技術
② 体内でカプセルを捕捉する技術
③ 捕捉されたカプセルを破壊する技術
④ 体内に注入されたカプセルのモニタリング技術

これまでの研究により、②では定在波を用いたマイクロカプセルの捕捉[7]~[9]、③では超音波の照射によるカプセルの崩壊[10]、さらには超音波音場内での気泡運動の観察や理論的考察[11]などが行われてきた。本研究室でも④の実現を目指し、超音波断層像の輝度情報からカプセル濃度を検出するシステムを開発[12]した。しかしながら、①に関しては体内に投与した後のカプセルは血流に任せるのみで、拡散によって目的部でのカプセル濃度は低くなるという問題が残っていた。

そこで我々は、分岐を有する模擬血管に超音波を照射することでカプセルに経路選択機能を付加できることを示し[13]、理論的検証を行った。本論文では超音波の音圧や、水流の流速などのパラメータ変化に伴うカプセル誘導の精度について光学的観測を行い、カプセルの誘導条件を算出した。

2. 実験方法

2−1　マイクロカプセルとその懸濁液

本研究ではマイクロカプセルとして、松本油脂社製マイクロスフェアーF-80Eを用いた。このカプセルは熱可塑性高分子（AN系コポリマー）の殻を有し、炭化水素（イソブタン）を内包している。生分解性が無いため生体で使用することは出来ないが、本研究で用いる音圧及び流速の範囲で安定であるため採用した。またカプセルの直径は、通常のマイクロバブルよりも１桁大きい63~75 μmに統一した。本来であれば、赤血球（直径約8 μm）程度のサイ

※本記事は第29回超音波シンポジウムで発表された論文に基づいております。

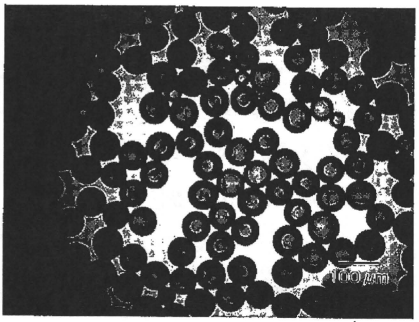

第1図　マイクロカプセルF-80Eの顕微鏡写真

ズを用いるべきであるが、後述する模擬血管の製作限界に対する顕微鏡の倍率との関係上、この範囲となった。カプセルの顕微鏡写真を第1図に示す。

マイクロスフェアーは粉体状で存在し、そのサイズは30 μm以下のものから120 μm程度のものまで含まれる。そこでカプセルを水に溶かし、目開き各38、63、75、90 μmの篩（ふるい）を用いてカプセルサイズを選別した。

2−2　水流中のカプセルに対する音響作用力

マイクロサイズのカプセルやバブルは内部に気体を含むため、超音波照射下で膨張収縮運動（体積振動）を行う。この体積振動とカプセル付近の音圧勾配の積の時間平均によりカプセルが超音波から受ける音響放射力が決まる。一般的に、音響放射力とはカプセルを定在波の腹や節に捕捉する力、進行波によってビーム方向へ移動させる力である。そしてこの力は水流中を流れるマイクロカプセルにも作用し、第2図に示すように超音波の照射方向にカプセルを移動させることが出来ると考えられる。

音響放射力Facは、式(1)で表される。

$$F_{ac}=\frac{4}{3}\pi R_0^3 A\frac{P_A^2}{\rho c^2} \qquad \cdots(1)$$

ここでρは媒質の密度、cは音速、P_Aは音圧、R_0はカプセル径、Aは定数である。流路内では、カプセルはストークスの法則より得られる水流からの抗力を受けるため、音響放射力の発生方向に、ストークス抵抗に逆らいながら第2図に示すように移動すると考えられる。

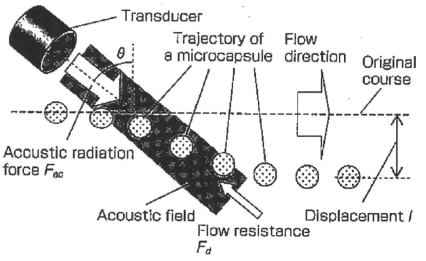

第2図　超音波照射下で流体中に存在するマイクロカプセルの軌跡

2−3　模擬血管とカプセルの挙動観察法

実験に用いる模擬血管として、超音波透過性に優れたポリエチレングリコールを用いて外形80×50×15 mmの直方体を作成し、その内部に第3図のように内径2 mmで1：2のY字型分岐を形成した。分岐部における超音波照射下のカプセル挙動を観察するために、図中のobserved area 1を倒立顕微鏡(DMIRB, LEICA社製）で観測する実験系を構築した。

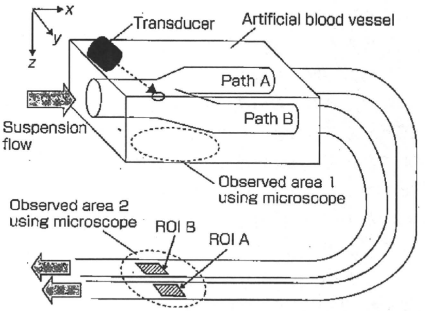

第3図　Y字分岐を有する模擬血管とトランスデューサの配置

この実験系を用いて分岐部を流れるカプセルの挙動を顕微鏡に接続した高速度カメラで観察した。超音波の発生は、ファンクションジェネレータにより発生させた正弦波を高周波増幅器で増幅し、中心周波数1 MHzの集束型超音波トランスデューサから照射した。また65〜73 μmのカプセルの共振周波数は約100 kHz前後であり、これによって超音波照射によるカプセル崩壊の可能性は小さい。また超音波の音圧と水流の流速の範囲は、120〜160 kPa、100〜

250 mm/sとした。

2−4 模擬血管の分岐部に対する超音波照射法

トランスデューサは直径25 mmの円筒形で、照射面から中心軸上45 mmの位置で放射音圧が最大（半値幅約3 mm）となることから、トランスデューサの設置は模擬血管の流路との距離を45 mmに保つことにした。超音波を照射する地点は第4図に示す各地点で、模擬血管の中心軸交点をO地点とし、この点を基準にP、Q、Rを1 mm間隔に決定した。そしてO〜Rの各地点を中心としてトランスデューサをy-z平面に対して50°と固定し、さらにx-y平面上のトランスデューサの設置角度θを−50〜80°まで変化させた。また超音波照射地点の変更は、照射角度を決めた後にx-yステージを用いて行った。

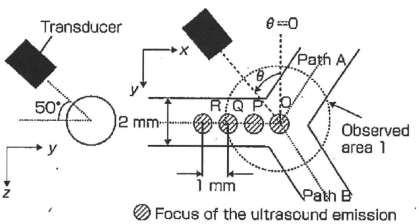

第4図 模擬血管に対する超音波の照射方法

ここで流速100 mm/sで流路を流れる直径65〜73 μmのカプセル懸濁液に対して、音圧160 kPaで周波数1 MHzの正弦波の集束超音波を第4図のQ地点にθ=60°で照射した時のobserved area 1の連続写真を第5図に示す。(a)はカプセル懸濁液を注入直後で、各写真の時間間隔は1 secである。カプセルは流路壁面に押さえつけられ、流路B側に誘導される様子が観察された。この現象は超音波の照射を停止するとほぼ同時に確認されなくなった。そのためカプセル誘導が音響放射力によって起こされたことが確認された。

2−5 流路を流れるカプセル量の評価

前述の実験系で示した分岐部を観察するだけでは、定量的なカプセル量を計測できない。そこで第3図に示した模擬血管の分岐後に外径2 mm，内径1 mmの半透明なチューブを接続して延長し、分岐点の下流300 mmの下流地点をobserved area 2とし、流路が平行になるように配置した。observed area 2の観測画面を第6図に示す。流路A、Bを通過するカプセルの計測法として、第6図に示される撮影範囲内に、同じ大きさの2つの関心領域を設定し、カプセルを流していない状態の画像の関心領域内における輝度平均値と比較した。具体的には、カプセルを流す前の関心領域の輝度平均値をREFとし、カプセルが流れている間の輝度平均値との差を式(2)のように計算し、REFとの比をShadow indexとして次式のように定義した。

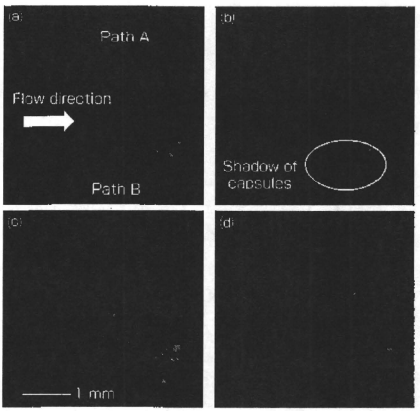

第6図 Observed area 1で観察できるマイクロカプセルの誘導

$$\sigma=\left(REF-\sum_{x}\sum_{y}f(x,y)\right)/REF \qquad \cdots(2)$$

ただし、fは画素の輝度値であり、ROI A、Bそれぞれに Shadow indexを計測した。この値はカプセル懸濁液の濃度と流速に依存するため、条件を固

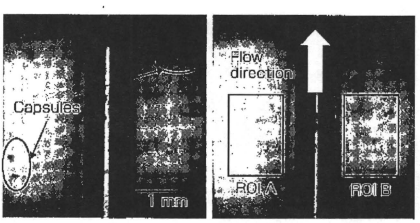

(a) 超音波照射なし　(b) 超音波照射あり

第6図 Observed area 2におけるマイクロカプセル濃度の計測

定する必要があるが、検証の結果、カプセル濃度が0.15～0.25 g/Lの範囲で300 mm/s以下の流速であれば、Shadow indexの変化を顕著に捉えられることが分かった[04]。よって以後の実験は濃度0.2 g/Lのカプセル懸濁液を用いて実験を行った。

3. カプセル誘導実験とその結果

3－1 超音波の照射位置・角度変化に対するカプセル誘導性能

流速100 mm/sで流路を流れるカプセルに対して、周波数1 MHz、音圧160 kPaの超音波を第4図に示す模擬血管の分岐部O～R地点に照射した。超音波の照射位置と角度によって、両流路へ流れるカプセル量に差があることが観測されたため、ROI BのShadow indexからROI AのShadow indexを減算することにより、流路B方向へ誘導されるカプセル量を評価した。その結果を第7図に示す。

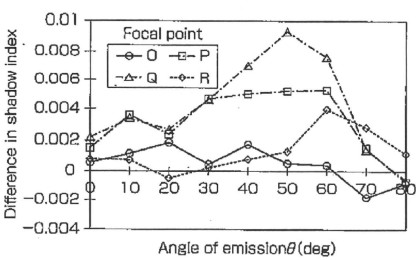

第7図 流路の分岐部への照射超音波の角度とカプセル誘導効率の関係
(流速100 mm/s、周波数1 MHz、音圧160 kPa)

この結果より、最も効率良く分岐部でカプセルを誘導するためには、超音波の焦点をQ、照射角度θ＝50°にした時であった。また焦点を分岐点（O）にすると、どの角度から超音波を照射してもカプセルを誘導することは出来なくなった。また上記の傾向は、超音波の照射を、流路AとBを逆にしても同様であった。これよりカプセル誘導を効率よく行うためには、超音波の照射位置と角度が重要であることが示唆された。

3－2 音圧・流速変化によるカプセル誘導実験

前節にて導出した条件（焦点Q, θ＝50°）を固定し、音圧と流速を変化させてカプセル誘導性能を比較した。第8図に流速を100 mm/sに固定し、音圧を変化させたときの結果を、また第9図に音圧を160 kPaに固定し、流速を変化させたときの結果を示す。両図とも、棒グラフはShadow index値を、折れ線グラフは計算によって求めたカプセル移動距離（第2図）[04]を示す。

この結果より周波数1 MHzの超音波でカプセル誘導を実現するためには、約150 kPa以上の音圧で150 mm/s以下の流速が必要なことが明らかとなった。

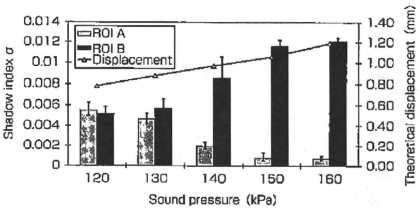

第8図 照射超音波の音圧の変化に対するROI A及びBにおけるShadow index の変化
(周波数1 MHz、流速100 mm/s)

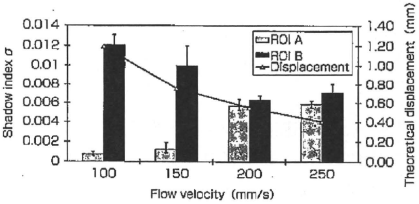

第9図 流速の変化に対するROI A及びBにおけるShadow indexの変化
(周波数1 MHz、焦点音圧160 kPa)

4. 実験結果に対する考察

3－1節の結果より、カプセルを分岐部で誘導するためには、超音波の照射位置と角度が重要な要因であることが示された。そこでカプセル誘導が可能であった時の超音波の音場分布を分岐部に重ねてみると、カプセル誘導が可能となる超音波の照射方法は、誘導する流路と超音波の進行方向が交差する場合であった。このことから流路分岐部でカプセルを誘導するための条件は、分岐前の地点と目的流路の両方の領域を超音波が通過する事と考えられた。

また3－2節の実験より、160 kPa程度の高音圧であればカプセルの誘導が可能であり、音圧を下げるに従いカプセルの誘導精度が落ちていることがわかる。これは音響放射力が小さくなるため、カプセルを目的の流路に移動させることが出来ないためと考えられる。一方、流速が速くなるに従って、カプセルが音場領域を通過する時間が短くなる。そのため、カプセルが受ける音響放射力の影響が小さくなり、カプセルの誘導が起こり難くなると考えられる。

また本研究の実験で使用した最大音圧は160 kPaであるが、この程度であればMI値は0.16程度となり、安全上の問題はない。最後にカプセルのサイズに関しては、今回は63～75 μmを使用したが、生体応用を考えるとこのサイズでは抹消血管を通過できない。音響放射力は式(1)に示すようにカプセルの体積に比例するため、生体内で使用可能な赤血球サイズのカプセルを使用する場合、カプセル径が約1/8になるため、音響放射力は1/500程度になると考えられる。しかしこの技術の最終目標はカテーテルの到達が困難な抹消血管であり、その血流は数mm/sと考えられる。今回は100 mm/s～250 mm/sの範囲の流速を用いたため、カプセルサイズを小さくすることによって音響放射力が低下した場合でも、同様の現象を起こす条件は導出可能と考えられる。

5. おわりに

本研究では、マイクロカプセルを用いた超音波DDS実現のため、体外からの超音波照射により分岐部を流れるカプセルの能動的流路選択の可能性について検討を行った。その結果、超音波の照射によって誘導される様子が観察された。そして流路分岐部にてカプセルを誘導するために必要な条件は、誘導する流路と超音波の進行方向が交差することである。今後は複雑な分岐部でもカプセルを誘導できる条件を数学的モデルによって確立することを目指す。

＜参考文献＞

(1) 橋田充："ドラッグデリバリシステム－創薬と治療への新たなる挑戦－"、化学同人（1995）
(2) 石原謙：BME、Vol.6、No.1、pp.45-52（1992）
(3) 山田正敏・田畑泰彦：生体医工学、Vol.43、No.2、pp.238-246（2005）
(4) 工藤信樹・栗林香織・名取道也・森安史典・山本克之：電子情報通信学会論文誌A、Vol.J84A、No.12、pp.1492-1499（2001）
(5) 立花克郎：生体医工学、Vol.43、No.2、pp.211-215（2005）
(6) T.Makuta, F.Takemura：Physics of Fluids, Vol.18, No.10, 108102（2006）
(7) T.Lilliehorn, U.Simu, M.Nilsson, M.Almqvist, T.Stepinski, T.Laurell, J.Nilsson, and S.Johansson：Ultrasonics, Vol.43, No.5, pp.293-303（2005）
(8) Y.Yamakoshi and M.Koganezawa：Jpn. J. Appl. Phys., Vol.44, No.6B, 4583-4587（2005）
(9) 小塚晃透：日本音響学会誌、Vol.61、No.3、pp.154-159（2005）
(10) D.Koyama, A.Osaki, W.Kiyan and Y.Watanabe：IEEE Trans. Ultrason, Ferroelect, Freq. Contr., Vol.53, No.7, 1314-1321（2006）
(11) 工藤信樹・平尾紀文・岡田健吾・山本克之：電子情報通信学会和文誌、Vol.J89A、No.9、pp.746-753（2006）
(12) 桝田晃司・村松悠佑・濱部一行・石原謙：生体医工学、Vol.46、No.2、pp.275-282（2008）
(13) Y.Muramatsu, S.Ueda, R.Nakamoto, Y.Nakayashiki, K.Masuda and K.Ishihara：Proc. of 4th European Medical & Biological Engineering Conference, pp.1589-1593（2008）
(14) K.Masuda, Y.Muramatsu, S.Ueda, R.Nakamoto, Y.Nakayashiki, and K.Ishihara：Jpn. J. Appl. Phys., Vol.48, No.7, 07GK03（2009）

【筆者紹介】

村松　悠佑
東京農工大学　大学院　生物システム応用科学府
生物システム応用科学専攻　博士前期課程修了
〒184-8588　東京都小金井市中町2-24-16
TEL：042-388-7130　FAX：042-388-7219

桝田　晃司
東京農工大学　大学院　生物システム応用科学府
准教授
〒184-8588　東京都小金井市中町2-24-16
TEL：042-388-7130　FAX：042-388-7219

32nd Annual International Conference of the IEEE EMBS
Buenos Aires, Argentina, August 31 - September 4, 2010

Study to prevent the Density of Microcapsules from diffusing in Blood Vessel by Local Acoustic Radiation Force

Kohji Masuda, *Member, IEEE*, Nobuyuki Watarai, Ryusuke Nakamoto, Yoshitaka Miyamoto, Keri Kim and Toshio Chiba

***Abstract*— We have already reported our attempt to constrain direction of microcapsules in flow owing to an acoustic radiation force. However, the diameter of capsules was too large not to be applied *in vivo*. Furthermore, acoustic radiation force affected only in focal area because focused ultrasound was used. Thus we have improved our experiment by using microcapsules as small as blood cells and introducing a plane wave of ultrasound. We prepared an artificial blood vessel including a Y-form bifurcation established two observation areas. Then we newly defined the induction index to evaluate the difference of capsule density in two paths of downstream. As the result, optimum angle of ultrasound emission to induce to desired path was derived. And the induction index increased in proportion to the central frequency of ultrasound, which is affected by forming aggregation of capsules to receive more radiation force.**

I. Introduction

MANY researches of drug delivery system (DDS) have been proposed by applying microcapsules or microbubbles as a drug carrier in human body [1-3]. The existence of capsules (or bubbles) improves the introduction efficiency to affect the target area by making use of sonoporation [4]. While the lifetime of the microbubbles is several minutes, we consider the microcapsules are better for use with various types of delivery. However, because of the diffusion of capsules after injection, it is difficult to deliver capsules from the point of injection to desired target area through bifurcations of blood vessel. If the behavior of capsules could be controlled and constrained the direction, the introduction efficiency would be enhanced. Owing to an acoustic radiation force [5-7], which is a physical phenomenon where an acoustic wave pushes an obstacle along its direction of propagation, we have ever reported our attempt to propel microcapsules in water [8,9]. We have elucidated the conditions in sound pressure, flow velocity and diameter of capsules for active path selection of capsules in an artificial blood vessel. However, because we used capsules which diameters were ranged more than 60 μm, so that they were too great to be applied *in vivo*. Furthermore, we also used focused ultrasound to concentrate acoustic radiation force, which affected only in focal area. Because an acoustic radiation force is proportional to the cube of the size of a capsule, larger acoustic field can produce more radiation force to propel a capsule in flow. Thus we have improved our experiment to adopt capsules as small as blood cells with a plane wave of ultrasound.

Considering micrometer-sized microcapsules, upon ultrasound exposure, they are oscillated to produce Bjerknes force and to aggregate each other [10] if the frequency of ultrasound is near their resonance frequency. We already confirmed aggregation of capsules in a straight flow when acoustic radiation force was produced in oncoming direction with MHz-order frequencies [8]. However, frequency dependence had not been elucidated when capsules were propelled in flow by the radiation force [11,12]. In this paper we investigated optimal condition to propel microcapsules in flow using plane wave of ultrasound with various frequencies.

II. Principle

Assuming that the shape of capsules is sphere and they are located in uniform acoustic field, an acoustic radiation force acts to propel a capsule in the direction of acoustic propagation. And when the microcapsules are placed in flow, a capsule should receive a flow resistance. If the acoustic radiation force is greater than the flow resistance, the trajectory of the capsule is curved, as shown in Fig.1.

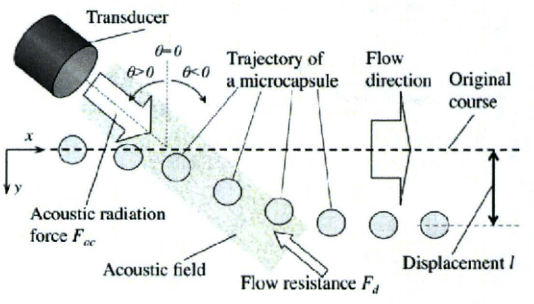

Fig.1. Trajectory of microcapsule in flow under ultrasound emission.

At a positive value of angle θ in Fig.1, a capsule is propelled to y-direction with lower flow resistance than at a negative value of angle θ. At larger absolute of angle θ, though a capsule passes through the acoustic field for a longer period, radiation force operates a capsule to propel in

Manuscript received April 1, 2010. This work was supported in part by Health Labor Sciences Research Grant 200813004A.

Kohji Masuda, Nobuyuki Watarai and Ryusuke Nakamoto are with Graduate School of Bio-Applications and Systems Engineering, Tokyo University of Agriculture and Technology, Koganei, Tokyo, 184-8588 Japan (e-mail: masuda_k@cc.tuat.ac.jp).

Yoshitaka Miyamoto is with School of Medicine, Nagoya University, Nagoya, 466-8550 Japan.

Keri Kim and Toshio Chiba is with National Center for Child Health and Development, Tokyo, 157-8535 Japan

x-direction more than in y-direction. In Fig.1, although the shape of the acoustic field is expressed as a square, it is measured before the experiment. Here the acoustic radiation force is expressed as per the following equation [12,13]

$$F_{ac} = \pi r^2 Y_p P, \qquad (1)$$

where P is the mean energy density of the incident wave, Y_p is a dimensionless factor called radiation force function that depends on the scattering and absorption properties of the capsule and r is the radius of the capsule. Since Y_p does not include an item of frequency [14], it is valuable to investigate the effect of ultrasound frequency in F_{ac}.

III. Experiments

A. Diameter distribution of microcapsules

We used the F-04E microcapsule (Matsumoto Oil), which has a shell made of polyvinyl chloride (PVC), a specific gravity of 0.0225, and an average diameter of 4 μm. It contains isobutene inside and is stable in room temperature. We selected only those microcapsules with a diameter less than 5 μm by using micro sieves. We measured the diameter of more than 800 capsules through five microscope images to elucidate the diameter distribution of capsules. Figure 2 shows the diameter distribution of capsules as bars, where diameters of capsules between 2 and 3.5 μm are mostly included. Since the solid line in Fig.2 indicates the resonance frequency f of microbubble, which is calculated as per eq. (2) [6], the resonance frequency is ranged between 2 and 4 MHz according to the diameter.

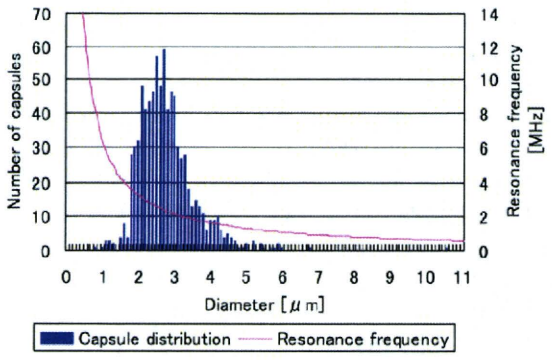

Fig. 2. The diameter distribution of F-04E microcapsules plotted with the resonance frequency of eq.(2) according to the diameter.

$$f = \frac{1}{2\pi r}\sqrt{\frac{3kP}{\rho}}, \qquad (2)$$

where k is the ratio of specific heats. However, because of the shell, the resonance frequency of microcapsules should be higher than that of microbubbles. According to a mathematical simulation [15], theoretical resonance frequency of microcapsules is estimated between 5 and 7 MHz with the diameter of 4 μm. Thus the behavior of capsules is considered to be mostly affected by MHz-order frequencies.

B. Observation of capsule behavior

We also have prepared an artificial blood vessel made of polyethylene glycol (PEG), including a Y-form bifurcation, as shown in the schematic view of Fig. 3. The external size was 85 x 55 x 10 mm^3 and inner diameter of the paths was 2 mm. The blood vessel was placed in the bottom of a water tank, which was filled with water. Because the acoustic impedance of PEG (sound velocity: 1540-1560 m/s, density: 1.27g/mL) is similar to that of water, the energy of ultrasound in water reaches the path with high efficiency. As shown in Fig.3, optical images of the observed areas 1 and 2 were recorded independently using a microscope (Omron, KH-7700) and an inverted microscope (Leica, DMRIB), respectively.

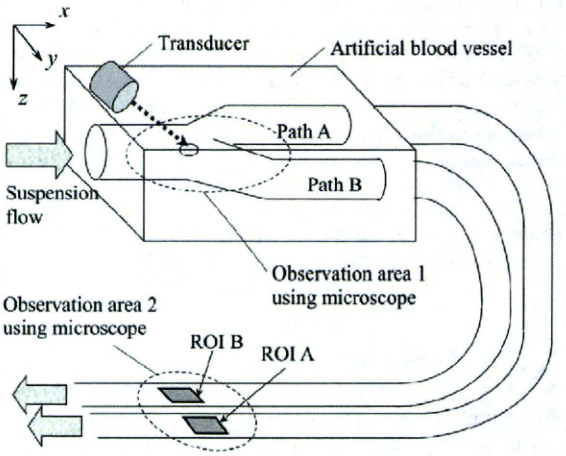

Fig.3. Schematic view of artificial blood vessel with the location of two observation areas.

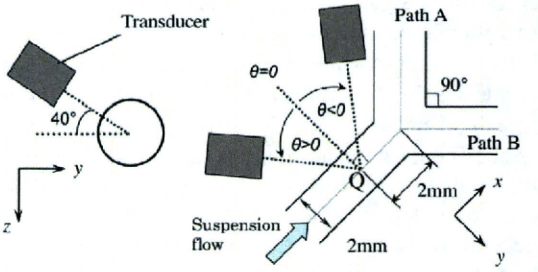

Fig.4. Position configuration between a transducer and the artificial blood vessel near the bifurcation.

Figure 4 shows the position configuration between a transducer and the artificial blood vessel near the bifurcation in the observed area 1. The axis of the transducer was set at 40 degrees from −y direction around the x-axis to prevent physical interference between the transducer and the edge of the water tank. The transducer included a flat ceramic disc with a diameter of 20 mm to emit plane wave of ultrasound. We have prepared five transducers, which have their center frequencies as 0.5, 1, 2, 3 and 5 MHz, respectively, to compare the effect between near and far from resonance frequencies. Measuring two-dimensional distribution of sound pressure in above five transducers, the half width of

ultrasound beam is ranged between 4 and 5 mm. Therefore the axis of the transducer was directed to the point Q, as shown in Fig. 4, which was set to be 2 mm from the bifurcation point to upstream course to adjust angle θ deg to the z-axis. The distance of the surface of a transducer from the point Q was set as between 50 and 60 mm so that the point Q is included in the area of highest sound pressure.

C. *Evaluation of induction of capsules to the desired path*

As shown in Fig.5, when ultrasound was emitted, aggregations of capsules were clearly observed to enter path B rather than A in the observation area 1, whereas neither aggregations of capsules nor significant difference between paths were observed without ultrasound. To evaluate the number of capsules that passed through each path, we extended the two paths using semitransparent tubes and established an observed area 2, where both paths were observable in a single view. Figure 6 shows microscope images of the observed area 2, which were captured using a high-speed camera (Casio, EX-F1) attached to the microscope with an interval time of 3.3 ms (300 fps), when capsule suspension was injected with flow velocity of 5 mm/s with ultrasound emission of 2 MHz and maximum sound pressure of 500 kPa. Because of the limitation of optical magnification, though individual microcapsules cannot be distinguished, thicker suspension was confirmed.

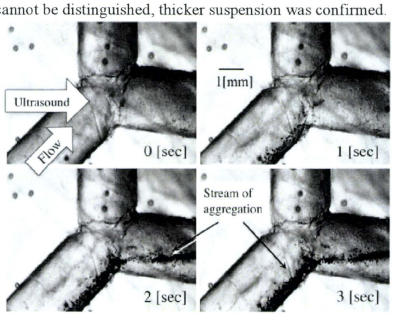

Fig.5.Transition of microscope images of observation area 1 after injection of capsule suspension (flow velocity: 20 mm/s, center frequency of ultrasound: 2 MHz and maximum sound pressure: 400 kPa).

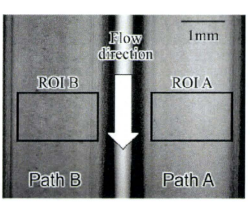

Fig.6. Microscope images of observation area 2, which was taken at 300 fps after injection of capsule suspension in flow velocity 5 mm/s with ultrasound emission of 2 MHz and maximum sound pressure as 500 kPa.

To measure amount of microcapsules, we established two square regions of interest (ROI), which size is 1.8 x 1.2 mm2, in each path (ROIs A and B) and calculated the average brightness. In the previous paper [8,9] we have evaluated amount of capsules by defining shadow index, which reflects brightness change according to existence of capsules in a ROI. However, the value of the shadow index cannot be compared between ROIs if there is initial brightness difference between them. Thus we newly defined the induction index by comparing two ROIs as follows.

Figure 7 shows variations of brightness average in both ROIs upon injection of a capsule suspension with flow velocity of 20 mm/s. Before the injection, brightness was constant but there was a difference between two ROIs. According to the appearance of capsules, after 7 s, brightness of both ROIs decreased simultaneously. A significant different variation was confirmed upon ultrasound emission of 2 MHz and 500 kPa, which indicates more capsules were induced to ROI B after 28 s. And according to disappearance of capsules, after 48 s, they returned to their initial brightness. Thus calculating the subtraction of brightness with capsules from initial brightness in each ROI, and comparing between ROIs, we have defined the induction index ξ_B of capsules to be induced to the path B rather than the path A using the following equation.

$$\xi_B = \frac{(I_B - I_{B0}) - (I_A - I_{A0})}{(I_B - I_{B0}) + (I_A - I_{A0})} \times 100 \ [\%], \quad (3)$$

where I_{A0} and I_{B0} indicate initial brightness average without capsules, and I_A and I_B indicate brightness average with capsules, in the ROI A and B, respectively. We confirmed that the induction index ξ_B reflects the relative ratio of capsules to pass ROI B versus total amount of capsules through our previously recorded movies [8,9] which calculated shadow index versus capsules density.

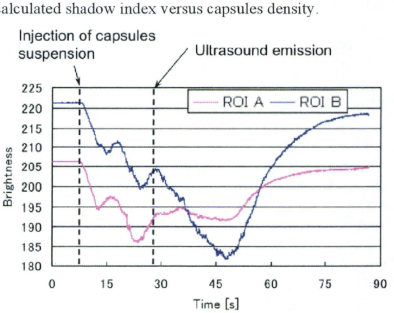

Fig.7. Variations of brightness average in ROIs A and B upon injection of a capsule suspension with flow velocity of 20 mm/s, before and after ultrasound emission of maximum sound pressure of 500 kPa and center frequency of 2 MHz.

IV. Results

Figure 8 shows the induction index ξ_B versus the angle of ultrasound emission θ for five kinds of maximum sound pressure, flow velocity of 20 mm/s and center frequency of 3 MHz. Here the value of induction index was calculated from the sampled frames recorded with high frame of 300 fps, while capsules were appeared in the frame under ultrasound emission. The number of sampled frames was set up to 300 frames, which depends on the duration of capsules appearance. When the sound pressure is less than 200 kPa, dominant induction to path B was observed in the positive angle of emission. When the sound pressure is more than 300 kPa, though capsule induction to path B was confirmed at angle of emission of -60 degree, significant induction to path B was confirmed at angle of emission of 30 degree. The optimum angle of ultrasound emission for induction to path B in the experiment was at an angle of 30 degree, which was used in the following experiment.

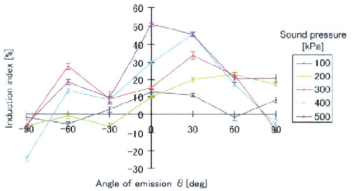

Fig.8. Induction index versus angle of emission with plane ultrasound of 3 MHz and flow velocity of 20 mm/s.

We measured the induction index upon emission of sinusoidal ultrasound with a frequency of 0.5, 1, 2, 3 and 5 MHz. Figure 9 shows the values of induction index versus the maximum sound pressure, where θ was fixed as 30 degree, when a flow velocity ranged as 20 mm/s. The induction index increased in proportion not only to the sound pressure but also to the central frequency of ultrasound. Regarding the central frequency, more capsules were induced to the desired path when it was close to the resonance frequency, which is supposed to be more than 5 MHz. We have considered that the result reflects the effect of aggregation of capsules.

Because capsules form aggregations under ultrasound emission, they should be equivalent to larger volume than isolated capsules. When the frequency is near resonance frequency, the capsules would be greatly oscillated to form larger aggregation and to receive more acoustic radiation force to the direction of propagation. We have to investigate behavior of capsules more precisely under various conditions of ultrasound.

From those results, using the higher pressure, higher frequency and plane ultrasound, the more capsules could be inducted to the desired path at the bifurcation of blood vessel. In the next step we are going to establish the behavior of capsules in flow theoretically before applying to *in vivo* experiment. The effect of acoustic streaming should be considered by using higher frequency than 5 MHz. Meanwhile we are going to develop a method to identify the precise location of bifurcations *in vivo* by detecting and constructing three-dimensional shape of the blood vessel.

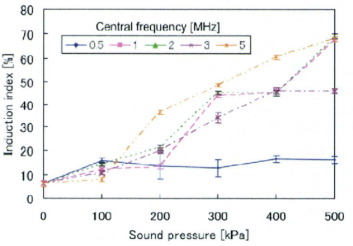

Fig.9. Induction index versus maximum sound pressure of plane ultrasound by the angle of emission of 30 deg in flow velocity of 20 mm/s.

V. Conclusions

In this study, we realized active control of microcapsules with a diameter less than 5 μm to constrain the direction in an artificial blood vessel. In a simple bifurcation, significant induction was confirmed when the angle of ultrasound emission was 30 degree from the rectangular of the flow to upstream. We confirmed that capsules were induced into the desired path using the higher pressure, higher frequency and plane ultrasound. For further analysis, the precise conditions necessary to realize active control of capsules in a complicated shape of blood vessel should be elucidated. Also we are going to consider applications for the future *in vivo* experiments.

References

[1] N.de Jong, R.Cornet, and C.T.Lancée: Ultrasonics 32 (1994) 447-453.
[2] K.Okada, N.Kudo, K.Niwa, and K.Yamamoto: J. Med. Ultrason. 32 (2005) 3-11.
[3] H.Zheng, P.Dayton, C.Caskey, S.Zhao, S.Qin, and K.Ferrara: Ultrasound in Med. & Biol., 33 (2007) 1978-1987.
[4] Y.Yamakoshi, Y. Koitabashi, N. Nakajima and T. Miwa: Jpn. J. Appl. Phys. 45 (2006) 4712-4717.
[5] J.J.Rychak, A.L.Klibanov, J.A.Hossack: IEEE Trans. Ultrason, Ferroelec. and Freq. Control, 52 (2005) 421-433.
[6] H.Mitome: Jpn. J. Appl. Phys. 40 (2001) 3484-3487.
[7] T. Kozuka, K. Yasui, T. Tuziuti, A. Towata, J. Lee, and Y. Iida: Jpn. J. Appl. Phys. 48 (2009) 07GM09.
[8] K.Masuda, R.Nakamoto, Y.Muramatsu, Y.Miyamoto, K.Kim and T. Chiba: Proc. of 31st Annual Intl Conf. IEEE EMBS (2009) 295-298.
[9] K.Masuda, Y.Muramatsu, S.Ueda, R.Nakamoto, Y.Nakayashiki, and K. Ishihara: Jpn. J. Appl. Phys. 48 (2009) 07GK03.
[10] Y. Yamakoshi and T. Miwa: Jpn. J. Appl. Phys. 47 (2008) 4127-4131.
[11] T. Lilliehorn, U. Simu, M. Nilsson, M. Almqvist, T. Stepinski, T. Laurell, J. Nilsson, and S. Johansson: Ultrasonics 43 (2005) 293-303.
[12] T.Hasegawa, Y.Hino, A.Annou, H.Noda, and M.Kato: J. Acoust. Soc. Am. 93 (1993) 154-161.
[13] F. G. Mitri: Wave motion 43 (2005) 12-19.
[14] T.Hasegawa, T.Kido, C.W.Min, T.Iizuka, and C.Matsuoka: Acoust. Sci. & Tech. 22 (2001) 273-281.
[15] K.Yasui, J.Lee, T.Tuziuti, A.Towata, T.Kozuka, and Y.Iida: J. Acoust. Soc. Am. 126 (2009) 973-982.

Ultrasound -Assisted Gene Transfer to Adipose Tissue-Derived Stem/Progenitor Cells (ASCs)

Yoshitaka Miyamoto[a, b], Hitomi Ueno[b], Rei Hokari[b], Wenji Yuan[b], Shuichi Kuno[b], Takashi Kakimoto[b], Shin Enosawa[c], Yoichi Negishi[d], Kiyoshi Yoshinaka[e], Yoichiro Matsumoto[e], Toshio Chiba[b], and Shuji Hayashi[a]

[a]*Department of Advanced Medicine in Biotechnology and Robotics, Nagoya University Graduate School of Medicine, Higashi-ku, Nagoya 461-0047, Japan.*
[b]*Department of Clinical Research & Development, National Center for Child Health and Development, Tokyo, Japan.*
[c]*Department of Innovative Surgery, National Research Institute for Child Health and Development, Tokyo, Japan.*
[d]*Department of Drug and Gene Delivery System, School of Pharmacy, Tokyo University of Pharmacy and Life Science, Hachioji, Tokyo, Japan.*
[e]*Department of Mechanical Engineering, The University of Tokyo, Tokyo, Japan.*

Abstract. In recent years, multilineage adipose tissue-derived stem cells (ASCs) have become increasingly attractive as a promising source for cell transplantation and regenerative medicine. Particular interest has been expressed in the potential to make tissue stem cells, such as ASCs and marrow stromal cells (MSCs), differentiate by gene transfection. Gene transfection using highly efficient viral vectors such as adeno- and sendai viruses have been developed for this purpose. Sonoporation, or ultrasound (US)-assisted gene transfer, is an alternative gene manipulation technique which employs the creation of a jet stream by ultrasonic microbubble cavitation. Sonoporation using non-viral vectors is expected to be a much safer, although less efficient, tool for prospective clinical gene therapy. In this report, we assessed the efficacy of the sonoporation technique for gene transfer to ASCs. We isolated and cultured adipocyets from mouse adipose tissue. ASCs that have the potential to differentiate with transformation into adipocytes or osteoblasts were obtained. Using the US-assisted system, plasmid DNA containing beta-galactosidase (beta-Gal) and green fluorescent protein (GFP) genes were transferred to the ASCs. For this purpose, a Sonopore 4000 (NEPAGENE Co.) and a Sonazoid (Daiichi Sankyo Co.) instrument were used in combination. ASCs were subjected to US (3.1 MHz, 50% duty cycle, burst rate 2.0 Hz, intensity 1.2 W/cm^2, exposure time 30 sec). We observed that the gene was more efficiently transferred with increased concentrations of plasmid DNA (5-150 μg/mL). However, further optimization of the US parameters is required, as the gene transfer efficiency was still relatively low. In conclusion, we herein demonstrate that a gene can be transferred to ASCs using our US-assisted system. In regenerative medicine, this system might resolve the current issues surrounding the use of viral vectors for gene transfer.

Keywords: adipose tissue-derived stem/progenitor cells (ASCs), adipo/osteogenic potential, sonoporation, microbubble, gene transfer.
PACS: 87.18.Ed, 87.17.Uv, 87.18.Hf, 92.40.vu, 87.14.Df

INTRODUCTION

In recent years, multilineage adipose tissue-derived stem cells (ASCs) have become increasingly attractive as a promising source for cell transplantation and regenerative medicine [1-2]. Particular interest has been expressed with regard to the possibility that stem cells, such as ASCs and marrow stromal cells (MSCs), can be made to differentiate into a number of different cell or tissue types by means of gene transfer. Gene transfection using highly efficient viral vectors [3], such as adeno- and sendai viruses, have been adopted for this purpose. Sonoporation, a form of ultrasound (US)-assisted gene transfer, is an alternative gene manipulation technique which employs the creation of a jet stream by ultrasonic microbubble cavitation [4-5]. Sonoporation using non-viral vectors is expected to be a much safer, although less efficient, tool for prospective clinical gene therapy. In this study, we assessed the efficacy of the sonoporation technique for gene transfer to ASCs.

ISOLATION AND CULTURE OF ASC_S

Subcutaneous adipose tissue was obtained from 8 week old adult mice (CLEA Japan, Inc. Meguro, Tokyo, Japan). A 0.5g specimen of adipose tissue was washed three times with Hank's balanced salt solution, cut finely, and digested with 1 ml of 1 mg/ml type I collagenase (Collagenase Type I, 274U/mg, Koken Co., Ltd., Tokyo, Japan) for 45 min in a 37°C water bath with reciprocal shaking. Cells obtained after filtering the digested tissue through 100μm meshes were suspended in Dulbecco's modified Eagle's medium (DMEM)/F12 containing 20% fetal bovine serum and centrifuged at 1,200 rpm for 5 min at room temperature, then the sedimentary cell layer was collected. Suspension and centrifugation of the sedimentary cells was repeated three times before the cells were plated in culture flasks.

For attached culture, 1×10^5 adipocytes (sedimentary cells) were seeded into a T-25 flask (NUNC) with DMEM/F12 containing 20% FBS, 100 U/ml penicillin and 100 μg/ml streptomycin at 37°C in a humidified atmosphere of 5% CO_2. After the cells attached and spread, they were passaged. This growth/passaging cycle was repeated twice.

Mouse ASCs were successfully cultured, forming confluent monolayers (FIGURE 1.a). The cells had both adipogenic (FIGURE 1.b, [6]) and osteogenic differentiation capabilities (FIGURE 1.c). These data suggest that the harvested cells included adipose tissue-derived stem cells.

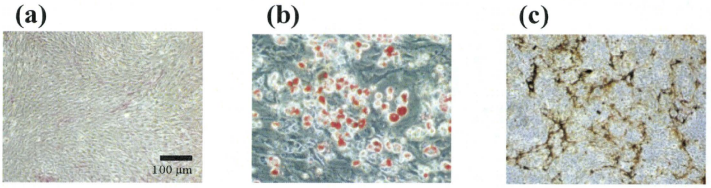

FIGURE 1. Adipo/osteogenic differentiation of ASCs. (a) The morphology of isolated and cultured ASCs. (b) Adipogenic differentiation of ASCs. The cells were stained with Oil Red O 1 week after adipogenic induction. (c) Osteogenic differentiation of ASCs. The cells were stained with Von Kossa stain 1 week after osteogenic induction. Scale bar, 100 μm.

US-ASSISTED GENE TRANSFER USING DIFFERENT METHODS

A total of 2×10^4 cells per well were grown in 96-well microplates. Following mixing of the microbubbles/DNA, the microplates were then subjected to ultrasound (frequency 3.1 MHz, duty cycle 50%, burst rate 2.0 Hz, intensity 1.27 W/cm^2, exposure time 30 sec) using a Sonopore 4000 (8 mm diameter probe; Nepa Gene Co. Ltd., Chiba, Japan). The CMV-LacZ cDNA plasmid was obtained from Clontech (Palo Alto, CA). DNA was used at a concentration of 20 μg/ml, and for transfer to the ASCs, 20μg/900μl of plasmid was mixed with a 100 μl volume of the sonazoid microbubbles (Daiichi Sankyo Corporation, Tokyo, Japan) to achieve a final concentration of 10% microbubbles.

Two methods were used for US exposure during the gene transfer tests (FIGURE 2). The first subjected the cells to the ultrasound on their attaching side (FIGURE 2, Method-1). For the second method, cells were subjected to ultrasound from the other side (FIGURE 2, Method-2). The microbubbles float on top as time passes. Therefore, compared to Method-1, the Method-2 approach results in a longer contact of microbubbles with the cells.

After the cells were transduced with the gene using ultrasound, they were incubated for 24 h and then assessed for their Lac Z gene expression. LacZ expression in the cells was detected by the X-gal staining method. The beta-galactosidase activity in the cells was detected as a method for evaluating gene transfer, thereby allowing for the easy identification of the cells expressing the Lac Z gene (X-Gal Staining Assay Kit (A10300K); Genlantis).

Although the samples showed no staining without sonazoid and/or US (FIGURE 3.a), they were positively stained when both 10% sonazoid and US were used (FIGURE 3.b and c). When Method-1 was used, the gene transfer efficiency was improved by reducing the amount (100-30μl) of the preparation solution in each well. Because the distance between the microbubbles and the attached cells is small, Method-1 is subject to sonoporation as well as Method-2. Therefore, we adopted

Method-1 because the experimental technique is simple and effective. The figure below shows both methods of gene transfer (FIGURE 2).

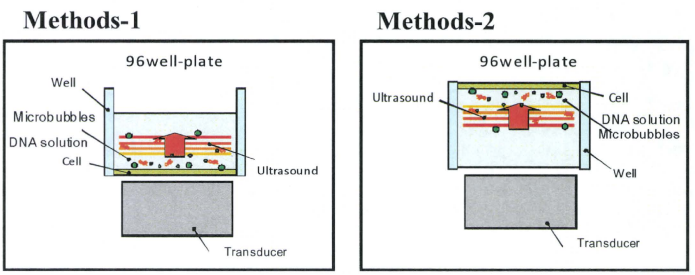

FIGURE 2. Two methods were used for US exposure. Methods-1: cells were subjected to ultrasound on the attaching side. Methods-2: cells were exposed to ultrasound from the other, non-attached, side.

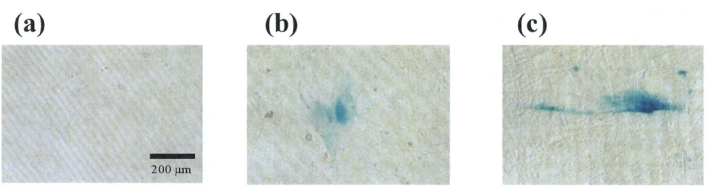

FIGURE 3. Microscopy after CMV-LacZ cDNA plasmid gene transfer. (a) Light microscopy of a normal control sample (with the Luc Z gene) without sonoporation. (b) Light microscopy revealed Luc Z expression after sonoporation with Luc Z genes and sonazoid using Methods-1. (c) Light microscopy revealed Luc Z expression after sonoporation with the Luc Z genes and sonazoid using Methods-2. Scale bar, 200 μm.

THE EFFECTS OF THE MICROBUBBLES

The cells (2×10^4 per well) were subjected to US (frequency 3.1 MHz, duty cycle 50%, burst rate 2.0 Hz, intensity 1.27 W/cm^2, exposure time 30 sec). We observed that the gene was more efficiently transferred with increased concentrations of sonazoid (0-40%). The effect of the microbubbles (sonazoid), and its effect on cell viability and cellular damage were analyzed by MTT assay using a Cell Counting Kit-8 (CCK-8; DOJINDO LABORATORIES, Kumamoto, Japan). Briefly, the CCK-8 reagent (10 μL) was added to each well and the reaction was allowed to occur for up to 2 hr. The absorption of the sample at 450 nm was measured against a background control, using a microplate reader. The cell number was counted after sonoporation.

The cell viability of ASCs before and after sonoporation was examined using a Cell Counting Kit-8 (FIGURE 4). After sonoporation with 10% sonazoid, the ASCs showed a lower viability compared to control ASCs and ASCs after sonoporation with 20-40% sonazoid. However, the cells most efficiently transferred the gene when the sonazoid concentration was 10% (data not shown). This confirmed that the ultrasonic microbubble cavitation occurred efficiently, therefore we then examined the impact of the concentrations of the GFP gene on the gene transfer efficiency.

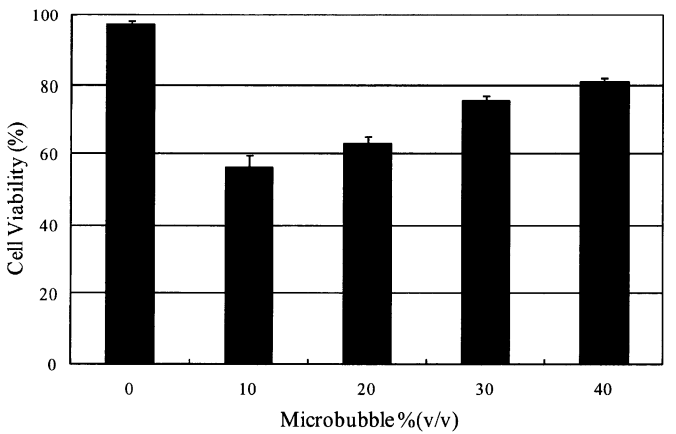

FIGURE 4. The viability of ASCs before/after sonoporation (0-40%). In these experiments, 2×10^4 cells per well were subjected to US (frequency 3.1 MHz, duty cycle 50%, burst rate 2.0 Hz, intensity 1.27 W/cm^2) for 30 sec.

US-ASSISTED GENE TRANSFER IN VITRO

In this series of experiments, 2×10^4 cells per well were subjected to US (frequency: 3.1 MHz, duty cycle: 50%, burst rate 2.0 Hz, intensity: 1.27 W/cm^2) for 30 sec. A green fluorescent protein (GFP)-encoding plasmid, pEGFP-N3, was obtained from Clontech (Palo Alto, CA). ASCs sonoporated with and without 10% sonazoid showed GFP expression after 24h by fluorescence microscopy (FIGURE 5).

Although the samples showed no expression of GFP when the ultrasound was applied without sonazoid (FIGURE 5.b, pEGFP-N3: 60 μg/ml), they did express GFP when both 10% sonazoid and US were used (FIGURE 5.c, pEGFP-N3: 60 μg/ml). The gene was more efficiently transferred with increased concentrations of the GFP gene (5-150 μg/ml, data not shown).